The CAF-1 complex couples Hippo pathway target gene expression and DNA replication

William B. Yee[a,b], Patrick M. Delaney[c], Pamela J. Vanderzalm[a,d], Srinivas Ramachandran[e,f,*], and Richard G. Fehon[a,b,*]

[a]Department of Molecular Genetics and Cell Biology, [b]Graduate Program in Cell and Molecular Biology, and [c]The College, The University of Chicago, Chicago, IL 60637; [d]Department of Biology, John Carroll University, University Heights, OH 44118; [e]RNA Bioscience Initiative and [f]Department of Biochemistry and Molecular Genetics, University of Colorado School of Medicine, Aurora, CO 80045

ABSTRACT **The Hippo signaling pathway regulates tissue growth and organ development in many animals, including humans. Pathway activity leads to inactivation of Yorkie (Yki), a transcriptional coactivator that drives expression of growth-promoting genes. In addition, Yki has been shown to recruit chromatin modifiers that enhance chromatin accessibility and thereby enhance Yki function. Here, we asked whether changes in chromatin accessibility that occur during DNA replication could also affect Yki function. We found that depletion of the chromatin assembly complex-1 (CAF-1) complex, a histone chaperone that is required for nucleosome assembly after DNA replication, in the wing imaginal epithelium leads to increased Hippo pathway target gene expression but does not affect expression of other genes. Yki shows greater association with target sites when CAF-1 is depleted and misregulation of target gene expression is Yki-dependent, suggesting that nucleosome assembly competes with Yki for pathway targets post-DNA replication. Consistent with this idea, increased target gene expression is DNA replication dependent and newly replicated chromatin at target sites shows marked nucleosome depletion when CAF-1 function is reduced. These observations suggest a connection between cell cycle progression and Hippo pathway target expression, providing insights into functions of the Hippo pathway in normal and abnormal tissue growth.**

Monitoring Editor
Tom Misteli
National Cancer Institute, NIH

Received: Jul 22, 2019
Revised: Sep 12, 2019
Accepted: Sep 19, 2019

INTRODUCTION

The Hippo signaling pathway regulates tissue growth and development by controlling proliferation and apoptosis (Pan, 2010). Central to the pathway is a multiple kinase cascade whose output is to phosphorylate Yorkie (Yki), a transcriptional coactivator (Huang *et al.*, 2005). Phosphorylated Yki is retained in the cytoplasm and is therefore transcriptionally inactive; in contrast, when the kinase pathway is inactive, Yki translocates into the nucleus to promote transcription of pathway target genes (Dong *et al.*, 2007; Oh and Irvine, 2008). Yki requires a DNA-binding partner such as Scalloped (Sd) to promote target gene transcription (Zhang *et al.*, 2008). When Yki is absent, Sd serves as a Hippo pathway target transcription repressor (Koontz *et al.*, 2013).

In addition to driving transcription by binding to DNA-binding partners, Yki is thought to recruit chromatin modifiers to regulate transcription. By mass spectrometry and coimmunoprecipitation, Yki was shown to physically interact with chromatin modifying factors including the GAGA factor and the Brahma complex (Oh *et al.*, 2013). More recently, Yki was shown to recruit the Trithorax-related (Trr) histone H3 lysine 4 (H3K4) methyltransferase complex through physically interacting with nuclear receptor coactivator 6 (Oh *et al.*, 2014; Qing *et al.*, 2014). These observations strongly suggest that Yki actively promotes changes in chromatin accessibility that in turn could

This article was published online ahead of print in MBoC in Press (http://www.molbiolcell.org/cgi/doi/10.1091/mbc.E19-07-0387) on September 25, 2019.

Author contributions: W.B.Y., P.J.V., S.R., and R.G.F. conceived and designed experiments; W.B.Y., P.M.D., P.J.V., and S.R. performed the experiments; W.B.Y., S.R., and R.G.F. analyzed the data; W.B.Y. and S.R. prepared the digital images; W.B.Y., S.R., and R.G.F. drafted the article.

*Address correspondence to: Richard G. Fehon (rfehon@uchicago.edu); Srinivas Ramachandran (srinivas.ramachandran@cuanschutz.edu).

Abbreviations used: CAF-1, chromatin assembly complex-1; ChIP, chromatin immunoprecipitation; Cora, Coracle; *dap*, *dacapo*; *Diap1*, death-associated inhibitor of apoptosis 1; Gapdh1, glyceraldehyde 3 phosphate dehydrogenase 1; H3K4, histone H3 lysine 4; Mcr, macroglobulin complement-related; *Mer*, Merlin; NDR, nucleosome-depleted region; ORC, origin replication complex; *Pdha*, *Pyruvate dehydrogenease E1 alpha subunit*; Sd, Scalloped; Trr, Trithorax-related; TSS, transcription start sites; Yki, Yorkie.

affect Hippo pathway target expression in different developmental contexts. Conversely, it is likely that chromatin accessibility regulates Yki binding and thus Hippo pathway target expression, but this has not been examined.

The chromatin assembly complex-1 (CAF-1) complex, which is composed of Caf1-180, Caf1-105, and Caf1-55 in *Drosophila*, is required for replication-coupled nucleosome assembly (Smith and Stillman, 1989). Specifically, the CAF-1 complex has been shown to interact with PCNA and to assemble H3 and H4 histones into newly synthesized DNA (Shibahara and Stillman, 1999). Consistent with this notion, recent work has shown that *Caf1-105* depletion in *Drosophila* S2 cells affects nucleosome deposition dynamics and chromatin accessibility of newly replicated chromatin (Ramachandran and Henikoff, 2016). In addition to its role as a histone chaperone, the CAF-1 complex also functions to maintain heterochromatin during DNA replication and restores nucleosomes on DNA after double-strand break repair (Murzina *et al.*, 1999; Moggs *et al.*, 2000). Together, these observations suggest that CAF-1 function can affect chromatin accessibility, particularly during DNA replication when genomic DNA is transiently free of nucleosomes or other binding factors. Interestingly, a recent study showed that loss of CAF-1 complex components results in increased expression of Notch signaling targets in actively replicating *Drosophila* follicle cells, raising the possibility that CAF-1 has functions that extend beyond post-DNA replication nucleosome assembly (Lo *et al.*, 2019).

In this study, we asked whether changes in chromatin accessibility associated with CAF-1 function during DNA replication might also affect Hippo pathway target expression. We show that depletion of CAF-1 complex components affects expression of Hippo pathway targets in a Yki-dependent manner, but does not affect expression of other genes not associated with Hippo signaling. Furthermore, we demonstrate that alteration of the CAF-1 complex affects Yki's accessibility to its target loci, and Hippo pathway target expression, in a DNA replication–dependent manner. Overall, our study uncovers a previously unknown link between DNA replication and Hippo pathway target expression through the CAF-1 complex.

RESULTS

Drosophila CAF-1 complex affects expression of Hippo pathway targets and growth

To ask whether changes in chromatin accessibility might affect Yki function, we investigated how depletion of the CAF-1 complex, which regulates post-DNA replication chromatin assembly (Shibahara and Stillman, 1999; Ramachandran and Henikoff, 2016), affects expression of known *yki* target genes. Like other upstream components of Hippo signaling, Merlin (*Mer*) has been shown to be a target for Yki transcriptional activation as a part of a negative feedback loop that regulates pathway activity (Hamaratoglu *et al.*, 2006). *Mer* has been extensively characterized in this context and therefore was used as a reporter for pathway activity in these studies.

We first observed that RNA interference (RNAi)-mediated depletion of *Caf1-180* using the *hh-Gal4* driver led to increased Mer accumulation as detected by antibody staining (Figure 1, A and A'). To determine whether the increased Mer staining we observed is due to increased *Mer* transcription, we performed in situ hybridization with a *Mer*-specific RNA probe and found that *Caf1-180* depletion led to increased *Mer* mRNA levels (Figure 1, B and B'; Supplemental Figure S1A).

To extend these initial observations, we asked whether *Caf1-180* depletion also affects the expression of other known Hippo pathway target genes (Figure 1, C–F'). In the wing disk, RNAi depletion of *Caf1-180* led to up-regulation of death-associated inhibitor of apoptosis 1 (*Diap1)-lacZ*^{j5C8} (*Diap1-lacZ*), a well-characterized Yki target (Zhang *et al.*, 2008). *Caf1-180* depletion also led to increased expression of *f-j5.1- LacZ (fj-lacZ)*, *ban3-GFP*, and CycE, three additional Hippo pathway targets (Huang *et al.*, 2005; Cho *et al.*, 2006; Sopko *et al.*, 2009; Matakatsu and Blair, 2012). Similar results were observed using nonoverlapping *Caf1-180* RNAi lines (Supplemental Figure S1, B–C''). Additionally, we made mitotic clones using the null *Caf1-180*^{270} allele and found that Mer staining and *fj-lacZ* reporter expression increased in the mutant clones, consistent with RNAi results (Figure 1, G–H''). Interestingly, *Caf1-180* depletion did not consistently cause increased *expanded* expression (Supplemental Figure S1, D–E'').

If *Caf1-180* depletion allows greater expression of *yki* target genes, then it also seems likely that *Caf1-180* depletion should result in tissue overgrowth. However, this prediction is nuanced by the fact that *Caf1-180* has an important role in postreplication chromatin assembly and therefore its loss should have pleiotropic and likely deleterious effects. Consistent with this notion, we found that strong RNAi-mediated *Caf1-180* depletion led to severe tissue loss (unpublished data), and *Caf1-180* mitotic mutant clones are noticeably smaller than their sister clones (Figure 1, G and H). For this reason, we used a weak Gal4 driver, *nubbin-Gal4* (*nub-Gal4*), to deplete *Caf1-180* moderately throughout the entire wing blade to assess its effect on growth. Under this driver wing imaginal disks expressing *Caf1-180* RNAi displayed significant overgrowth (Figure 1, I, J, and L). While these animals survived to the adult stage, their wings were severely misshapen (unpublished data).

Next, we asked whether *Caf1-180* affects Hippo pathway targets as part of the CAF-1 complex by asking whether depletion of the other subunits of the CAF-1 complex, Caf1-105 and Caf1-55, also affect Hippo pathway target expression. RNAi-mediated depletion of *Caf1-105 or Caf1-55* led to increased Mer, *Diap1-lacZ*, and *ban3-GFP* expression (Figure 1, M–O''). Consistent with experiments done with *hh-Gal4,* we conducted parallel experiments with *apterous-Gal4* (*ap-Gal4*) and obtained similar results (Supplemental Figure S1, F–H''). Taken together, our results showing that depletion of each of the three components of the CAF-1 complex led to up-regulation of Hippo pathway targets in a similar manner indicate that *Caf1-180* functions as a part of the CAF-1 complex to affect Hippo pathway target expression.

The CAF-1 complex preferentially affects Hippo pathway targets

Our observations that several characterized Hippo pathway targets are affected similarly by CAF-1 complex depletion raise the question of whether the CAF-1 complex preferentially affects Hippo pathway target expression or instead has a more general effect on transcription in the developing wing. To explore this possibility, we examined the effect of *Caf1-180* depletion on expression of genes that are not known to be regulated by Yki. Using available transcriptional reporters and antibodies, we found that *Caf1-180* depletion did not affect expression of Moesin (a protein that is structurally similar to Mer), *Dad-lacZ* (a target of BMP signaling; Figure 2, A–B''), Lamin, Macroglobulin complement-related (Mcr), Coracle (Cora), Diaphanous, beta-tubulin, or spaghetti squash (Supplemental Figure S2, A–F'). In contrast, as a control we consistently observed that *Caf1-180* depletion caused increased Mer staining in the same tissues.

To expand the number of testable targets and as a complementary approach to immunofluorescence staining, we used real time quantitative PCR (RT-qPCR) to examine the effect of *Caf1-180* depletion on Hippo pathway-related and -unrelated genes. Starting

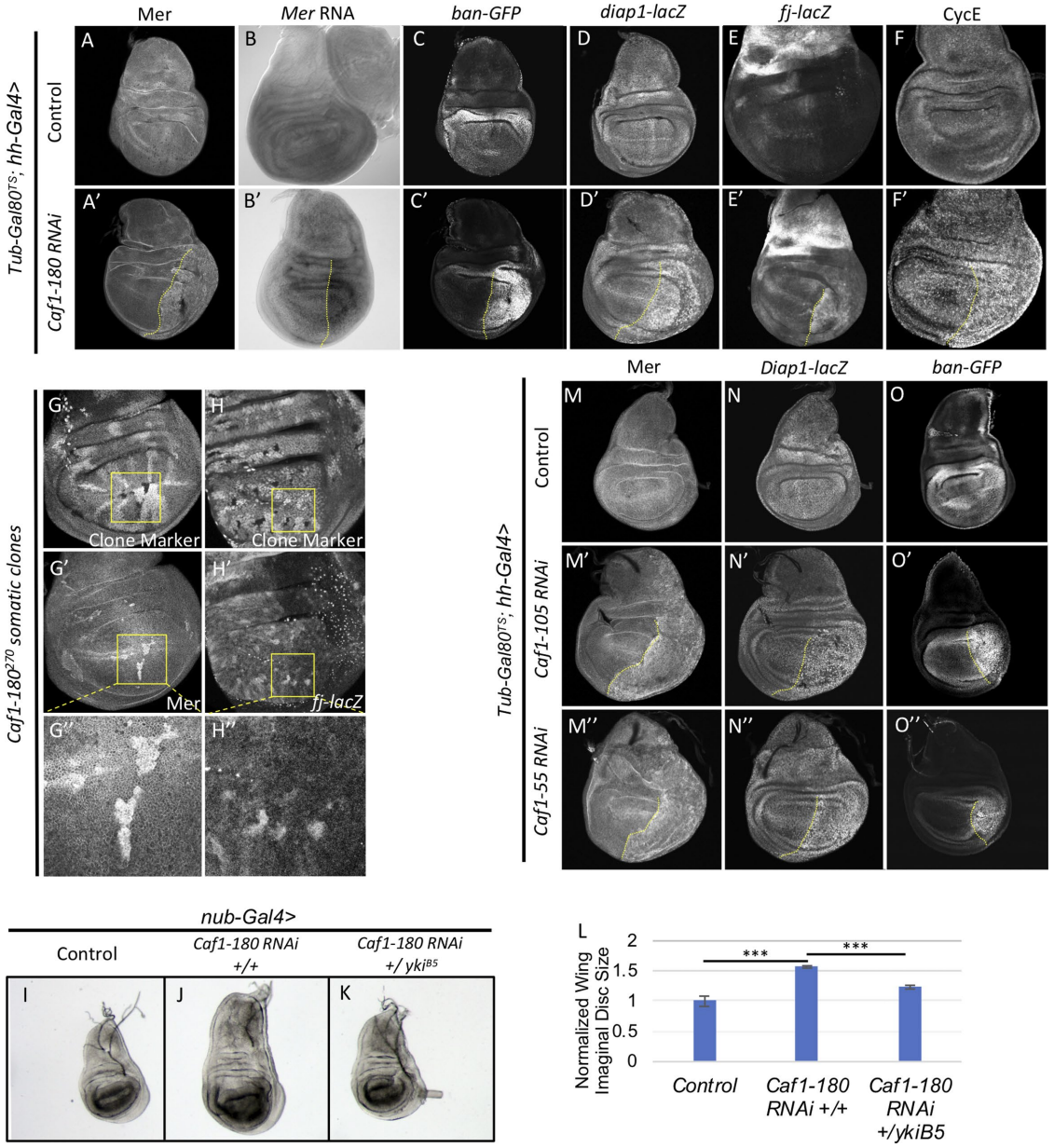

FIGURE 1: Loss of *Drosophila* CAF-1 increases Yki target gene expression. (A–F) *Caf1-180* depletion increases Yki target expression. Mer (A, A′), *Mer* (B, B′), *ban-GFP* (C, C′), *diap1-lacZ* (D, D′), *fj-lacZ* (E, E′), and CycE (F, F′) expression in control (A–F) and *Caf1-180* knockdown (A′–F′) wing disks. Larvae were incubated in restrictive temperature for 60 h before dissection. (G, H) Somatic mosaic mutant clones are marked by the absence of GFP (G, H). Loss of *Caf1-180* causes increased expression of the Yki targets Mer (G–G″) and *fj-lacZ* (H–H″) in *Caf1-180*^{270} clones. (I–L) *Caf1-180* depletion caused overgrowth. *Caf1-180* depletion throughout the wing blade under *nub-Gal4* leads to wing disk overgrowth (J, L). Removing one dose of *yki* partially suppresses the *Caf1-180* growth phenotype (K, L). In L, wing disk size is normalized to *nub-Gal4* control disks. Data are represented as mean ± SEM (***$p < 0.001$, Student's *t* test, $n = 12$ for each genotype). (M–O″) Depletion of other CAF-1 complex components also increases *yki* target expression. Mer (M–M″), *Diap1-lacZ* (N–N″), and *ban-GFP* (O–O″) expression in *Caf1-105* (M′, N′, O′) or *Caf1-55* (M″, N″, O″) depleted wing disks. Approximate location of the anterior–posterior expression boundary is marked by dashed yellow lines.

with known pathway targets, we first confirmed that *Mer, Diap1*, *ban*, and *CycE* transcript level increased in *Caf1-180*-depleted wing imaginal disks using a twofold increase as a threshold (Figure 2C). To examine CAF-1's effect beyond these well-characterized Hippo pathway targets, we examined additional Hippo pathway targets that were implicated from previous genome-wide studies (Oh *et al.*, 2013; Zhang *et al.*, 2017). We defined a set of high-confidence Yki targets as genes that were 1) up-regulated in *wts* depleted tissue, 2) up-regulated when *yki* is overexpressed, and 3) identified as Yki-binding targets in both ChiP and DamSeq data sets. We randomly selected 10 genes from this list and examined the effect of *Caf1-180* depletion on their expression (Figure 2D). Interestingly, *Caf1-180* depletion led to greater than twofold up-regulation of all but one of these genes. We then examined 15 genes that have not been

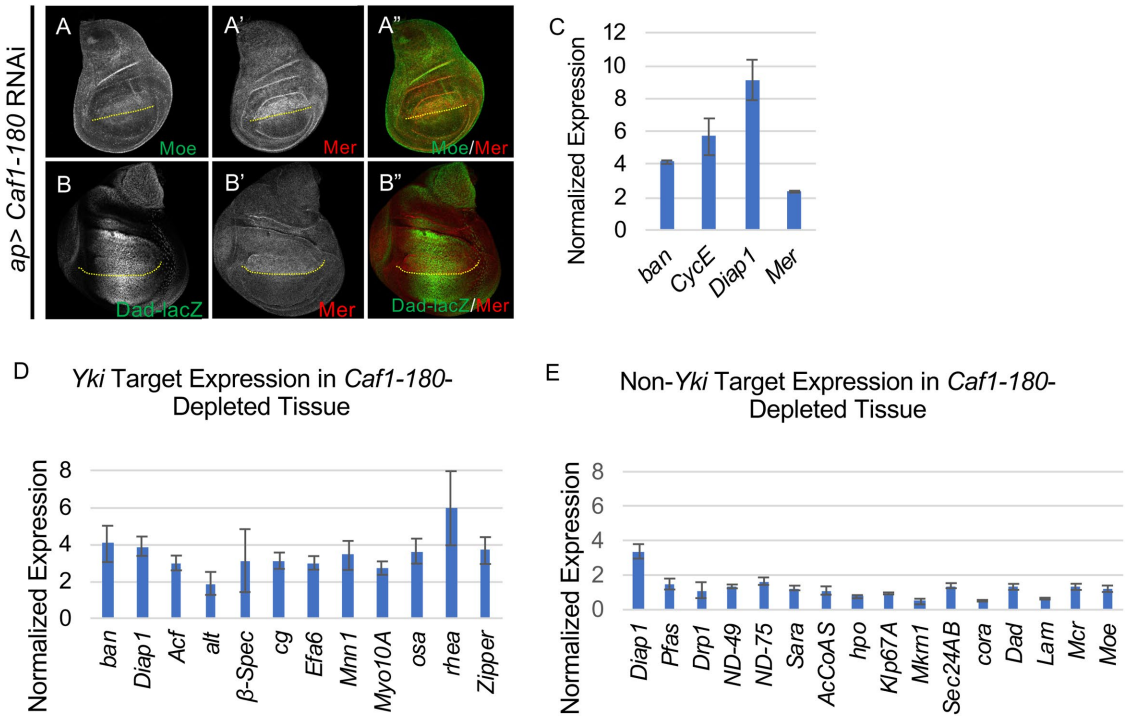

FIGURE 2: The CAF-1 complex preferentially affects Yki targets. (A–B") *Caf1-180* depletion did not change expression of representative non-Yki target genes. Moesin (A) and *Dad-lacZ* (B) expression was unaffected by *Caf1-180* knockdown under *ap-Gal4* in larval wing disks raised at 22°C. Mer staining (A', B') was used as control to confirm sufficient *Caf1-180* depletion. Approximate location of the dorsal-ventral expression boundary is marked by dashed yellow lines. (C–E) qPCR analysis of expression of Yki target genes (C, D) and nontargets (E). Data are represented as normalized expression ± SEM from two (E) or three (C, D) independent replicates. The threshold for up-regulation is a twofold increase. *Gapdh2, aTub84B,* and *Ubi-p63E* were used as normalization genes. While well-validated Yki targets (C) and a selected set of high-confidence targets (D, see text for description) were consistently up-regulated, a set of nontargets (E) was not.

implicated as Hippo pathway targets (Figure 2E). Using the twofold cutoff, *Caf1-180* depletion did not lead to up-regulation of any these genes. Collectively, our data strongly suggest that the CAF-1 complex preferentially affects Hippo pathway targets.

An explanation for increased *yki* target gene expression on *Caf1-180* depletion is that *Caf1-180* normally promotes Hippo pathway function through an unknown mechanism and thereby reduces Yki nuclear localization and transcriptional function. To test this idea, we asked whether depleting *Caf1-180* affects the subcellular localization of endogenously expressed Yki-YFP, which we previous have shown acts as a biosensor for Hippo pathway kinase activity (Xu *et al.*, 2018). We found no change in Yki-YFP's localization or abundance (Supplemental Figure S2, G and G') on *Caf1-180* depletion, suggesting that depletion of the *Caf1-180* does not affect activity the Hippo pathway kinase cascade and instead acts at the level of Yki itself.

The CAF-1 complex affects Hippo pathway target expression through Yki

The CAF-1 complex is thought to limit chromatin accessibility by promoting nucleosome deposition behind replication forks in S-phase nuclei (Kaufman *et al.*, 1995). Given this, we wondered whether the effect of CAF-1 complex component depletion on Hippo pathway target gene expression might reflect changes in accessibility of Yki to its target loci on chromatin. As an initial test of this idea, we examined how simultaneously depleting CAF-1 complex components and *yki* would affect Hippo pathway targets. Since *yki* is an essential gene for growth in the wing imaginal disk, we transiently depleted *yki* using *hh-Gal4* in combination with *Tub-Gal80^{TS}*, which allows Gal4-driven expression only at restrictive temperature, for 48 h before tissue collection. Using Mer staining as a readout of Hippo pathway target expression, depletion of *yki* alone had no discernable effect while, as expected, depletion of *Caf1-180* resulted in a dramatic increase in Mer staining (Figure 3, A–C). Interestingly, codepletion of *yki* strongly attenuated the effect of *Caf1-180* depletion on *Mer* expression (Figure 3D). Similarly, codepletion of *yki* reduced the effect of *Caf1-105*-depletion on *Mer* expression (Figure 3, E and F). Additionally, codepletion of *yki* and *Caf1-180* or *Caf1-105* suppressed *Diap1-lacZ* up-regulation caused by depletion of *Caf1-180* or *Caf1-105* alone (Figure 3, G–M).

The observation that codepletion of CAF-1 components and Yki suppressed expression of Yki target genes raises the question of whether overgrowth induced by *Caf1-180* RNAi (Figure 1, I and J) also requires Yki. To test this, we depleted *Caf1-180* in animals heterozygous for a *yki* null allele (*yki^{B5}*) (Huang *et al.*, 2005). Reduction in *yki* dosage substantially suppressed the *Caf1-180* RNAi phenotype in the wing imaginal disk (Figure 1, K and L). Collectively, the above data suggest that the CAF-1 complex affects Hippo pathway target expression in a *yki*-dependent manner.

The CAF-1 complex restricts Yki's interaction with Hippo pathway target loci

One possible explanation for the increased expression of *yki* regulated genes we observed is that Yki has greater access to its target loci when the CAF-1 complex is depleted. To test this idea, we conducted chromatin immunoprecipitation (ChIP) experiments to

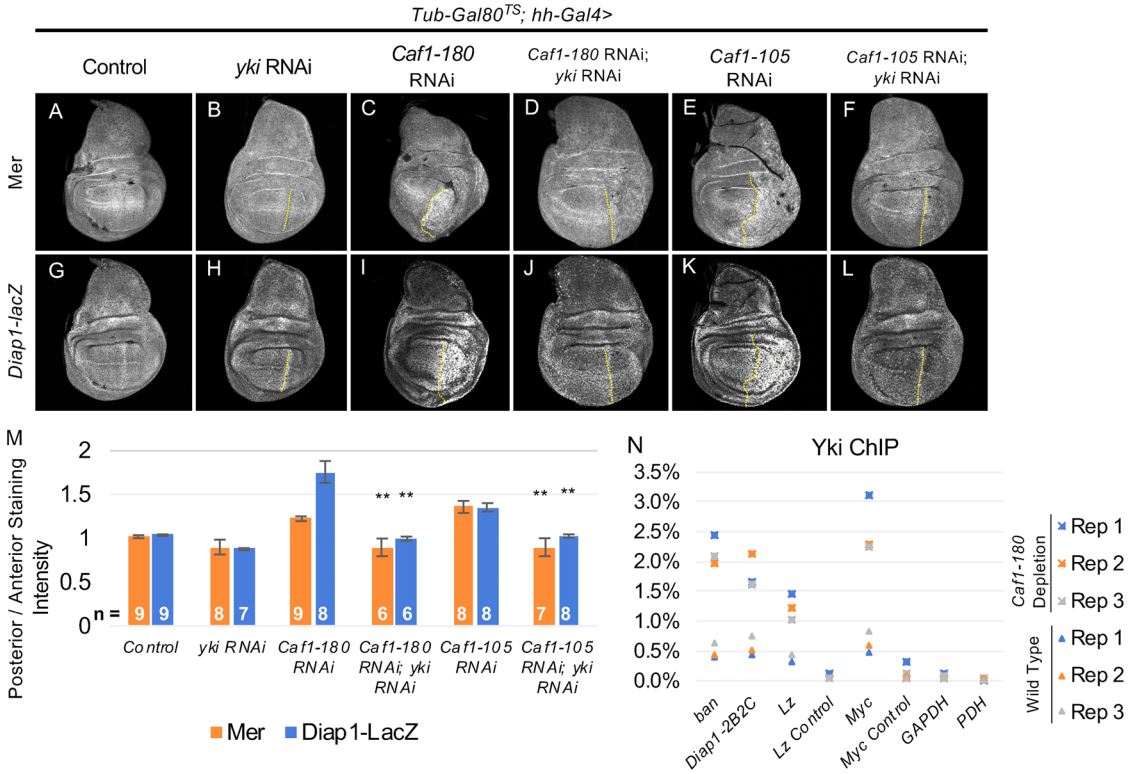

FIGURE 3: Yki is required for up-regulation of Hippo target gene expression under CAF-1 depletion. (A–L) Wing imaginal disks showing expression of Mer (A–F) and *diap1-lacZ* (G–L) expression in the indicated genotypes. Note that the target gene up-regulation caused by *Caf1-180* depletion is strongly suppressed by codepletion of *yki*. Larvae were incubated in restrictive temperature for 48 h before dissection. Approximate location of the anterior–posterior expression boundary is marked by dashed yellow lines. (M) Quantification of fluorescence intensity, calculated as a ratio of posterior/anterior (*hh-Gal4*/wild type) staining, in the indicated genotypes. Bars show mean ± SEM (**$p < 0.01$ for comparison of the indicated genotype to *Caf1-180* or *Caf1-105* depletion alone, Student's *t* test, n = number of disks quantified). (N) *Caf1-180* depletion enhanced Yki binding to its target loci. ChIP data are represented as the percentage of input DNA. *Lz* and *Myc* controls are regions near their respective gene's regulatory regions and acts as negative controls. *Gapdh2* and *Pdha* provide additional negative controls. Three biological replicates are shown.

examine Yki occupancy on target loci comparing normal cells to those depleted for CAF-1 components. For these experiments, we used a YFP-tagged Yki transgene expressed under its endogenous promoter *{yki-YFP}* in the background of *yki*^{B5} (Su *et al.*, 2017; Xu *et al.*, 2018). Using anti-GFP antibodies, we could then efficiently immunoprecipitate Yki from different genotypes. Homozygous *{yki-YFP} yki*^{B5} flies show no growth defect and were compared with *{yki-YFP} yki*^{B5} animals in which the CAF-1 complex component *Caf1-180* was depleted using *nub-Gal4*. As negative controls, we used *Glyceraldehyde 3 phosphate dehydrogenase 1* (*Gapdh*1) and *Pyruvate dehydrogenease E1 alpha subunit* (*Pdha*), which should be expressed independently of Yki activity.

We first focused on two well-characterized *yki* target regulatory regions: *ban*, whose Yki regulatory region has been mapped and used for a similar ChIP assay (Parker and Struhl, 2015), and *Diap1*, which has a defined enhancer element, *2B2C* that is regulated by *yki* and *sd* (Huang *et al.*, 2005; Wu *et al.*, 2008; Zhang *et al.*, 2008; Koontz *et al.*, 2013). In *{yki-YFP} yki*^{B5} imaginal disks, sequences including the CATTCA motif of *ban*, to which Yki binds, were strongly enriched relative to the *Gapdh1* and *Pdha* negative controls (Figure 3N). Strikingly, in *Caf1-180*-depleted imaginal disks, Yki pulled down an average of 2.2% of the input chromatin at *ban*, an approximately fourfold enrichment over the *{yki-YFP} yki*^{B5} controls ($p < 0.01$, $n = 3$ independent experimental replicates). In a similar manner, Yki occupancy at the *Diap1-2B2C* target site increased approximately threefold, from an average of 0.57% of the input chromatin in control tissue to 1.80% in *Caf1-180*-depleted tissue (Figure 3N).

To extend these observations, we conducted parallel experiments on *Myc* and *lz*, two additional Hippo pathway targets with previously characterized Yki-binding sites (Neto-Silva *et al.*, 2010; Milton *et al.*, 2014). Both studies also identified adjacent control chromosomal regions that do not bind Yki. Consistent with the observations for *ban* and *Diap1*, we observed significantly increased Yki binding in response to *Caf1-180* depletion at the Yki-binding sites within the *Myc* and *lz* loci (Figure 3N). In contrast, in our experiments the control regions displayed ~10-fold less ChIP signal in Yki-YFP IP's compared with Yki-binding sites. Additionally, Yki binding at control regions was not significantly altered by *Caf1-180* depletion (the control loci, *Gapdh1* and *Pdha*, behaved similarly). Together, these experiments showed directly that *Caf1-180* depletion increases Yki binding to its targets, suggesting that the CAF-1 complex limits Yki's accessibility to chromatin at target loci and thus its ability to promote target transcription.

The ability of the CAF-1 complex to affect Hippo pathway target expression depends on DNA replication

In *Drosophila* S2 cells, histone occupancy is reestablished quickly after replication, in part due to the CAF-1 complex's chaperone function. Indeed, reducing the abundance of CAF-1 complex components impairs post–DNA replication chromatin reestablishment

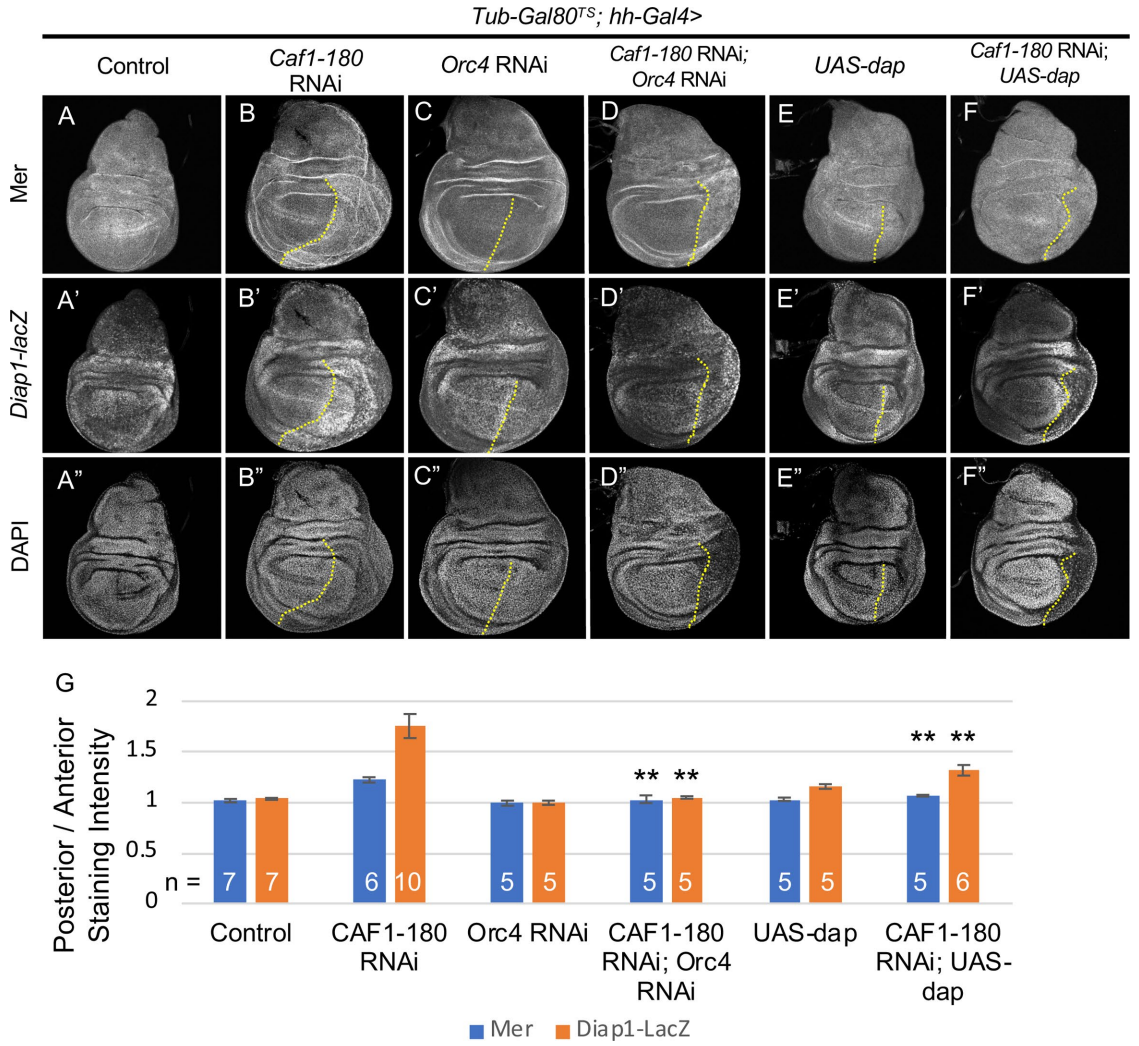

FIGURE 4: The relationship between DNA replication and Yki target gene expression. (A–F") *Orc4* depletion or *dap* expression attenuates Yki target up-regulation caused by *Caf1-180* depletion. Mer staining (A–F), *diap1-lacZ* expression (A'–F'), and DAPI staining (A"–F") in the indicated genotypes. DAPI staining shows reduced DNA in *Orc4* depleted (C", D") or *dap* expressing (E", F") wing disks. Larvae were incubated in restrictive temperature for 48 h before dissection. Approximate location of the anterior–posterior expression boundary is marked by dashed yellow lines. (G) Quantification of Yki target staining intensity in the indicated genotypes. Bars display ratios of posterior/anterior fluorescence intensity, represented as mean ± SEM (**$p < 0.01$ for comparison of the indicated genotype to *Caf1-180* depletion alone, Student's *t* test, *n* = number of disks quantified).

(Ramachandran and Henikoff, 2016). Given our results suggesting that Yki has greater access to its target sites when CAF-1 function is depleted, we wondered whether impairment of postreplication chromatin assembly might underlie Yki's increased accessibility to target loci. If so, then the increased Hippo pathway target expression we have observed in response to CAF-1 complex depletion should be DNA replication dependent.

To test whether the CAF-1 complex's ability to affect *Mer* expression depends on DNA replication, we asked whether simultaneously depleting *Caf1-180* and inhibiting DNA replication would suppress up-regulation of Mer or *Diap1-lacZ* staining characteristic of *Caf1-180* depletion alone. To inhibit DNA replication, we depleted Origin Replication Complex (ORC) components by RNAi. Although most available transgenic RNAi lines for other ORC components produce no observable phenotype when expressed in the wing using *hh-Gal4*, we found that depletion of *Orc4* using two nonoverlapping RNAi transgenes led to decreased 4',6-diamidino-2-phenylindole (DAPI) staining in the posterior compartment of the wing (Figure 4C" and Supplemental Figure S3, A–B') and pupal lethality or morphological defects (unpublished data), indicating that DNA replication was inhibited. Interestingly, while *Orc4* depletion alone had no effect on Mer or *Diap1-lacZ*, simultaneously depleting *Caf1-180* and *Orc4* attenuated *Mer* and *Diap1-lacZ* up-regulation compared with *Caf1-180* depletion alone (Figure 4, A–D" and G; Supplemental Figure S3, C–F).

As a second means of inhibiting DNA replication, we expressed *dacapo* (*dap*), a cell cycle regulator whose ectopic expression blocks cell cycle progression (De Nooij *et al.*, 1996). The *dap* expression using *hh-Gal4* also resulted in decreased DAPI staining, suggesting that DNA replication was slowed and had little or no effect on Mer or *Diap1-lacZ* level (Figure 4, E–E"). Consistent with experiments in which we depleted *Orc4*, simultaneously depleting *Caf1-180* and overexpressing *dap* suppressed the *Mer* and *Diap1-LacZ* up-regulation caused by *Caf1-180* depletion alone (Figure 4, E–G).

We also noticed that simultaneous depletion *Caf1-180* and *Orc4* (or coexpression of *dap*) resulted in synergistic undergrowth that was more substantial than *Caf1-180* depletion alone. This decreased cell

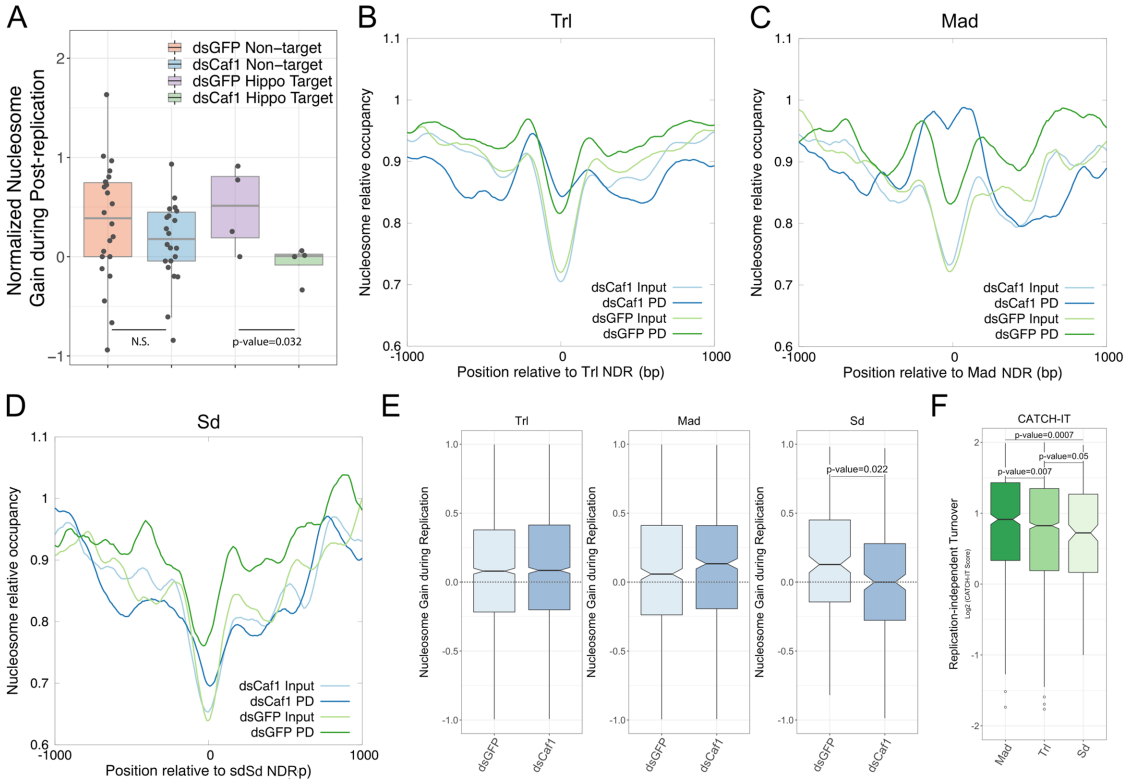

FIGURE 5: CAF-1–mediated nucleosome assembly dynamics for Yki target genes. (A) CAF-1 complex depletion impairs Yki target nucleosome deposition after DNA replication. Change in nucleosome occupancy at TSS ± 20 base pairs immediately postreplication was calculated by subtracting nucleosome occupancy at steady state from nucleosome occupancy postreplication determined by MINCE-seq; *p* value was calculated using a paired *t* test. (B–D) CAF-1 complex depletion impairs post–DNA replication nucleosome gain at Sd-binding sites. Average nucleosome profiles at Yki-binding sites with a Trl motif (B, $n = 2180$), Mad motif (C, $n = 736$), and Sd motif (D, $n = 270$). Here input refers to steady state nucleosome profile obtained from MINCE-seq and PD refers to newly replicated chromatin profiles obtained from MINCE-seq. (E) Change in nucleosome occupancy at binding site ± 50 base pairs immediately postreplication calculated by subtracting nucleosome occupancy at steady state from nucleosome occupancy postreplication determined by MINCE-seq. (F) Normalized CATCH-IT ratio at binding site ± 50 base pairs at Yki sites with Mad, Trl, and Sd motifs. NDR: nucleosome-depleted region (see *Materials and Methods*).

number was accompanied by a decrease in DAPI staining (Figure 4, D″ and F″), potentially complicating quantification of Yki target expression levels. To examine the possibility that codepletion of *Caf1-180* and *Orc4* nonspecifically decreases gene expression, we conducted parallel experiments on Mcr and Cora. We found that neither *Orc4* depletion alone or *Orc4* and *Caf1-180* codepletion affected Mcr (Supplemental Figure S3, G–I′) or Cora (Supplemental Figure S3, J–L′) abundance, suggesting that *Caf1-180* and *Orc4* specifically affected Hippo pathway targets. Collectively, our observation that inhibiting DNA replication suppressed the effect of *Caf1-180* depletion on Hippo pathway targets suggests that CAF-1 antagonizes Yki function in a DNA replication-dependent manner and is consistent with the idea that CAF-1–mediated nucleosome assembly after DNA replication inhibits the access of Yki to its target sites.

Differential timing of postreplication histone deposition may contribute to CAF-1's preferential effect at Yki targets

The CAF-1 complex is believed to function as a generic histone chaperone that deposits histone H3/H4 onto DNA behind the replication fork. However, the data presented here suggest that CAF-1 preferentially affects the expression of Hippo pathway targets in a Yki- and DNA replication–dependent manner. To explore how CAF-1 does this, we analyzed published MINCE-seq data from *Drosophila* S2 cells (Ramachandran and Henikoff, 2016) to see how nucleosome landscape changes postreplication at Yki targets. MINCE-seq is a metabolic labeling method that labels <10 kb of newly replicated chromatin for each active replication fork (with 10 min of labeling), followed by micrococcal nuclease treatment and DNA sequencing. Additionally, MINCE-seq can be used to profile nucleosomal footprints from both newly replicated and steady state chromatin from the same sample. In this study, MINCE-seq was also performed after knocking down CAF-1 to analyze changes in the nucleosome landscape behind the replication fork when replication-coupled nucleosome assembly was impaired (Ramachandran and Henikoff, 2016). We reanalyzed these data to compare nucleosome gains behind the replication fork for 22 genes (Figure 2E and Supplemental Table S1) that are not affected by CAF-1 knockdown to four genes (Figure 2C) that are up-regulated on *Caf1-180* knockdown in our experiments. We observed no significant change in nucleosome occupancy 10 min postreplication at the nontarget genes (Figure 5A) in response to CAF-1 depletion. However, we observed a strong impairment of nucleosome gain at transcription start sites (TSS) of the four verified Yki target genes.

To extend these observations, we sought to compare the behavior of different Yki-binding sites in response to CAF-1 depletion. Yki has been shown to bind to several DNA-binding proteins including Gaga factor (Trl), Mad, and Sd to activate specific genes (Wu *et al.*, 2008; Zhang *et al.*, 2008; Oh and Irvine, 2011). The direct effects of

the CAF-1 complex would manifest as nucleosomes replacing these DNA-binding proteins behind the replication fork, preventing Yki access to DNA postreplication. We asked which of the DNA-binding protein sites are most affected by CAF-1 knockdown. To do this, we identified the subset of all Yki ChIP sites from Oh *et al.* (2013) that had strong motifs for Trl, Mad, and Sd (Supplemental Table S2). When we plotted the average nucleosome landscape at steady state over sites of each transcription factor (TF), we observed nucleosome depletion (Figure 5, B–D, input data sets), pointing to TF binding. We then asked how this nucleosome landscape changes postreplication by plotting the average nucleosome landscape postreplication over sites of each (Figure 5, B–D, pull-down data sets). In controls (dsGFP), we observed nucleosome gain at Trl, Mad, and Sd sites postreplication (Figure 5, B–D). CAF-1 knockdown impaired postreplication nucleosome gains at Sd sites to a significant extent, while Trl and Mad sites instead appeared to show slight gains (Figure 5, B–D). To confirm these observations, we calculated net change in postreplication nucleosome occupancy for each binding site ±50 base pairs and plotted the distribution of the nucleosome occupancy (Figure 5E). We observed no difference or slight increase in nucleosome occupancy replication for Trl and Mad in CAF-1 knockdown cells compared with control, indicating that postreplication nucleosome dynamics at these sites are not affected by the absence of CAF-1. However, we observed a significant decrease in nucleosome gain postreplication at Sd sites on knockdown of CAF-1, indicating that Sd sites are highly sensitive to CAF-1 function postreplication.

A possible explanation for differential sensitivity to CAF-1 depletion at different binding sites is that CAF-1-independent nucleosome assembly also occurs postreplication at Trl and Mad sites (Ray-Gallet *et al.*, 2011), while Sd-binding sites are more dependent on CAF-1 for nucleosome deposition postreplication. Alternatively, if Trl and Mad sites have higher rates of nucleosome turnover throughout the cell cycle, nucleosome loss postreplication might be obscured. To explore this possibility, we calculated DNA replication-independent nucleosome turnover at Mad, Trl, and Sd sites using CATCH-IT (Teves and Henikoff, 2011) and found that Mad and Trl sites display significantly higher rates of replication-independent nucleosome turnover than observed at Sd sites (Figure 5F). Regardless of the precise mechanism, taken together these results suggest that Sd targets are protected by nucleosomes postreplication, and impairment of this process could allow Sd and its partner Yki to bind these genes postreplication.

The CAF-1 complex affects repressive histone modifications in a *yki*-dependent manner

Thus far, our data suggest that the CAF-1 complex influences Yki's accessibility to its target loci and as a result affects Yki target gene expression. We next explored how these seemingly transient changes in chromatin accessibility might lead to sustained changes in gene expression. In addition to driving transcription by interacting with DNA-binding partners such as Sd, recent studies showed that Yki can recruit activating chromatin modifiers such as Trr to increase chromatin accessibility at target sites (Oh *et al.*, 2013, 2014; Qing *et al.*, 2014). The observation that *Caf1-180* depletion causes greater Yki chromatin accessibility led us to wonder whether *Caf1-180* depletion might also affect chromatin activation through Yki.

Although Yki has a relatively small number of validated transcriptional targets, previous genome-wide studies have reported thousands of chromatin binding peaks, some of which colocalize with binding peaks of chromatin modifiers, including Trr (Oh *et al.*, 2013). This observation led us to wonder whether the effects of CAF-1 complex component depletion might have widespread effects on chromatin state. To assess this, we used antibodies against specific chromatin modifications to stain whole imaginal disks in which different CAF-1 components were depleted in a defined region of the tissue. A similar approach was used previously to assess the effects of Bre1 loss on H3K4 methylation (Xuan *et al.*, 2013). This approach allows side-by-side, internally controlled comparisons of staining in wild type and RNAi-depleted tissues. All of the antibodies used have been validated for immunofluorescence and to be specific for particular histone modifications (Subbanna *et al.*, 2013; Fei *et al.*, 2015; Rothbart *et al.*, 2015; Chiacchiera *et al.*, 2016; Le *et al.*, 2016).

Previous studies have shown that Yki can modulate H3K4 methylation, an activation mark, at the *diap1* and *ex* loci through its ability to recruit histone methyltransferases through interactions with NcoA6 (Oh *et al.*, 2014; Qing *et al.*, 2014). Therefore, we wondered whether the CAF-1 complex affects Hippo pathway target expression in part by preventing activating histone modifications such as H3K4 methylation. Using *hh-Gal4*, we depleted *Caf1-180* in the posterior compartment of the wing imaginal epithelium, leaving the anterior compartment as an internal control. As expected, antibody staining of imaginal disks using anti-H3K4me1 and anti-H3K4me3 resulted in distinctly nuclear staining. However, we found that *Caf1-180* depletion in the posterior of the wing did not noticeably affect staining for these activating marks when compared with anterior control cells (Supplemental Figure S4, A and B').

The CAF-1 complex also has been implicated in heterochromatin formation, which is thought to repress transcription by promoting the accumulation of repressive modifications (Huang *et al.*, 2010). For this reason, we next asked whether depletion of the CAF-1 complex might reduce repressive histone marks in the wing imaginal epithelium. We focused on H3K27 methylation, which is associated with repressed chromatin states and regulated by HP1 (Jamieson *et al.*, 2016), because *Caf1-180* was previously shown to affect HP1 dependent heterochromatin (Huang *et al.*, 2010).

To examine whether the CAF-1 complex affects H3K27 methylation, we depleted *Caf1-180,* again using the *hh-Gal4* driver and stained using H3K27me2- and H3K27me3-specific antibodies. Interestingly, *Caf1-180* depletion led to decreased staining of H3K27me2 and H3K27me3 (Figure 6, A–B" and G–H"), but in marked contrast did not reduce global histone H3 levels and instead led to moderately increased H3 staining (Supplemental Figure S4, C and C'). Previous work in mammalian cells has shown that under conditions of CAF-1 depletion, the HIRA complex functions in postreplication nucleosome assembly, replacing H3.1 with H3.3 (Ray-Gallet *et al.*, 2011). We speculate that the pan-H3 antibody we used has a preference for H3.3, resulting in greater staining under conditions of CAF-1 depletion.

The observation that *Caf1-180* depletion leads to decreased levels of the H3K27me2 and H3K27me3 chromatin modifications suggests two (not mutually exclusive) models: 1) that the CAF-1 complex promotes deposition of these repressive marks, or 2) that the increased binding of Yki to chromatin in response to CAF-1 depletion leads to decreased repressive marks. To address these possibilities, we reduced *yki* dosage in half ($yki^{B5}/+$) and again stained *Caf1-180*-depleted imaginal disks with modification-specific antibodies. We found that decreased *yki* dosage suppressed the effect of *Caf1-180* depletion on H3K27me2 and H3K27me3 staining (Figure 6, C–C", F, I–I", and L). This result suggests that Yki regulates transcription not only by promoting activating histone modifications but also by preventing repressive modifications. Consistent with published work (Huang *et al.*, 2010), we found that *Caf1-180* depletion decreased staining for H3K9 methylation

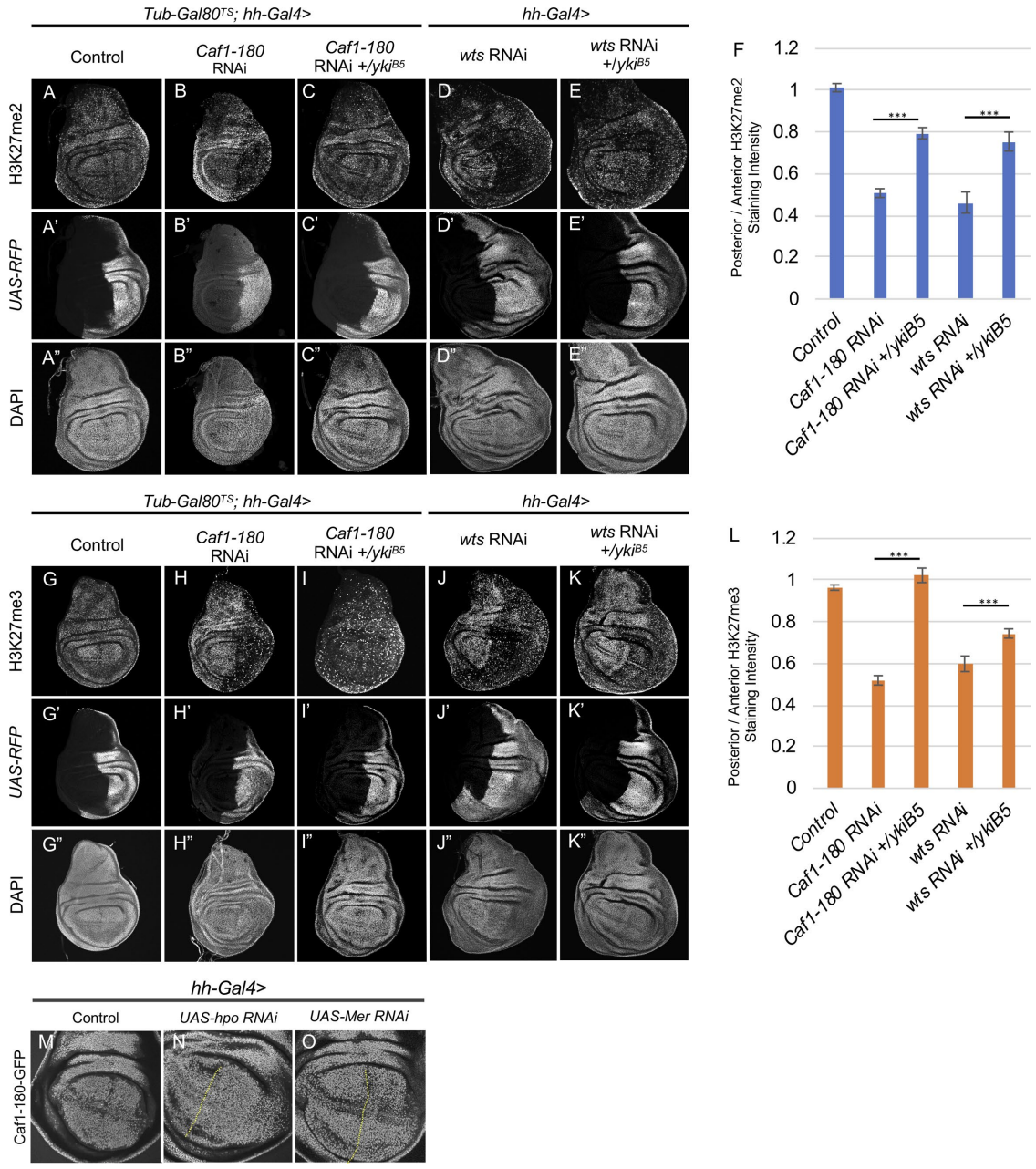

FIGURE 6: The CAF-1 complex and Hippo pathway components affect repressive histone marks in a Yki-dependent manner. (A–F) Mosaic wing imaginal disks of the indicated genotypes stained for H3K27me2. *Caf1-180* (B–B") or *wts* (D–D") depletion results in decreased H3K27me2 staining, while heterozygosity for *yki* (C–C", E–E") suppresses this effect. *UAS-RFP* marks the area of Gal4 expression and DAPI staining shows that decreased histone mark staining is not due to decreased DNA content. Quantification of H3K27me2 staining intensity (F) is shown as posterior/anterior ratios represented as mean ± SEM (***$p < 0.001$, Student's *t* test, $n = 10$ for each genotype). (G–L) Mosaic wing imaginal disks of the indicated genotypes stained for H3K27me3. As seen for H3K27me2, *Caf-180* (H-H") or *wts* (J–J") depletion results in decreased H3K27me3 staining, while heterozygosity for *yki* (I–I", K–K") suppresses this effect. Quantification of H3K27me3 staining intensity (L) is shown as posterior/anterior ratios represented as mean ± SEM (***$p < 0.001$, Student's *t* test, $n = 10$ for each genotype). (M–O) Hippo pathway component depletion did not affect Caf1-180 localization or abundance. Live imaging of Caf1-180-GFP in control (M), *hpo*-depleted (N), or *Mer*-depleted (O) wing imaginal disks. Note that *hpo*-depletion caused overgrowth of the posterior compartment in N. Approximate location of the anterior–posterior expression boundary is marked by dashed yellow lines.

(Supplemental Figure S4, D and D') and HP1 (Supplemental Figure S4, F–G'). Interestingly, the effect of *Caf1-180* depletion on H3K9 methylation was not *yki* dependent (Supplemental Figure S4, E and E') suggesting that the CAF-1 complex might regulate different histone modifications by different mechanisms.

To further examine the possibility that Yki can affect repressive chromatin modifications, we next asked whether activating Yki by attenuating Hippo pathway activity also affects repressive chromatin marks. In wing imaginal disks where *wts* was depleted by RNAi using *hh-Gal4*, we observed decreased H3K27me2 and H3K27me3

staining in the posterior compartment in comparison to the anterior compartment (Figure 6, D–D″, F, J–J″, and L). Similar results were observed with *hpo* depletion (Supplemental Figure S4, H and H′ and K–K′) and in *hpo* and *wts* mitotic clones (Supplemental Figure S4, L–O′″). To ask whether this decrease was Yki dependent, we reduced *yki* activity in the background of *hpo* or *wts* depletion and stained for H3K27me2 and H3K27me3. Interestingly, *wts* or *hpo* depletion in yki^{B5} heterozygotes displayed a significantly weaker effect on H3K27 methylation staining when compared with controls (Figure 6, E, F, K, and L; Supplemental Figure S4, H–K′). Collectively, these data strongly suggest that Yki can affect repressive histone marks, and that this activity can be regulated by Hippo signaling.

To address the possibility that Hippo pathway activity affects functioning of the CAF-1 complex, we used CRISPR–Cas9-based gene editing to insert *GFP* in-frame at the 3′ end of the *Caf1-180*'s coding sequence (*Caf1-180-GFP*). Homozygous *Caf1-180-GFP* animals showed normal growth and development, and *Caf1-180-GFP* was effectively depleted by *Caf1-180*-specific RNAi expression (Supplemental Figure S4, P–P″). However, depletion of *hpo* or *Mer* did not affect Caf1-180's localization or abundance (Figure 6, M–O). Likewise, *Mer* overexpression did not affect Caf1-180's abundance (Supplemental Figure S4, Q–Q″). Collectively, these data suggest that the CAF-1 complex function is not regulated by the Hippo pathway.

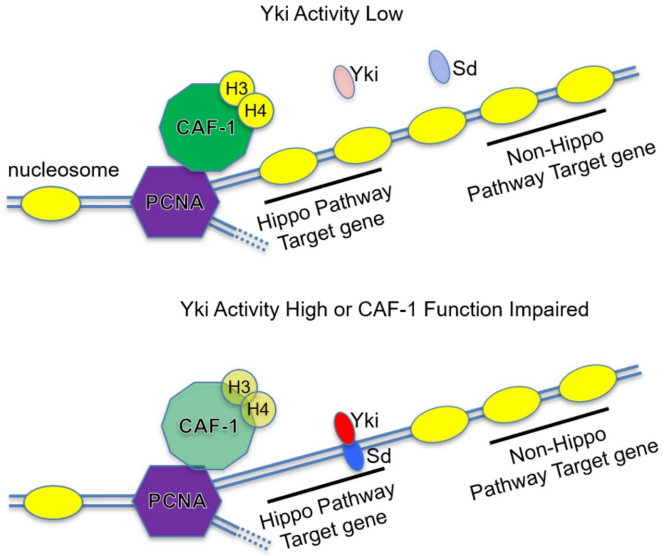

FIGURE 7: Model for how CAF-1 affects Yki target expression. At Sd/Yki targets, depletion of CAF-1 or, speculatively, under conditions of high Yki activity, Yki gains greater access to its binding sites after the replication fork passes. Increased Sd and Yki binding leads to increased transcription of Yki targets. See *Discussion* for details.

DISCUSSION

In this study, we have explored the functional relationship between CAF-1, a histone chaperone complex that assembles nucleosomes after DNA replication, and expression of Hippo pathway targets. We found that depletion of CAF-1 components leads to increased expression of Yki target genes in a Yki-dependent manner, that this effect depends on DNA replication, and that decreased CAF-1 function results in increased accessibility of Yki to its target loci. Our results further indicate that binding sites for Sd, the major DNA-binding cofactor for Yki-mediated transcription, display greater dependence on CAF-1 for nucleosome assembly after replication when compared with other TF-binding sites. We believe that as a consequence, depletion of CAF-1 complex components leads to increased Hippo pathway target expression, while not affecting expression of many nonpathway-related genes (Figure 7). Together, these observations reveal a previously uncharacterized role of the CAF-1 complex and a poorly understood mode of Yki target gene regulation.

Although initially it seems surprising that a ubiquitous nucleosome chaperone has relatively specific transcriptional effects, this is not the first example of CAF-1 mutations with specific developmental phenotypes. In *Caenorhabditis elegans,* CAF-1 mutations have been shown to disrupt the MI-e3D asymmetric cell fate decision in the nervous system resulting in extra e3D-like cells (Nakano *et al.*, 2011). This defect was attributed to altered postreplication nucleosome assembly, possibly relating to asymmetric nucleosome assembly on leading and lagging strands behind the replication fork. While we have no evidence from our studies suggesting replicative asymmetry, the notion that delayed nucleosome reassembly post-DNA replication results in altered transcription of specific genes is common to both cases. Additionally, recent work in mammalian cells has shown that the CAF-1 complex regulates pluripotency in adult cells by preferentially affecting *Sox2* binding to its target loci (Cheloufi *et al.*, 2015), and studies in *Drosophila* have shown that CAF-1 modulates expression of target genes downstream of Notch signaling (Yu *et al.*, 2013; Lo *et al.*, 2019). Taken together, these results highlight the interplay between assembly of nucleosomes and the assembly of TF complexes on newly replicated DNA in mitotically active cells.

What remains unclear is why certain transcriptional complexes, such as those associated with Yki and Notch signaling, seem to be particularly affected by competition with assembling nucleosomes. By examining the post–DNA replication nucleosome dynamics at the DNA-binding sites of three different Yki partners, Sd, Trl, and Mad, we found that nucleosome deposition is more severely affected by CAF-1 depletion at Sd-binding sites than at the binding sites of the other Yki partners. This observation suggests that Sd-binding sites are more dependent on CAF-1 for postreplication nucleosome assembly. Additionally, we found that replication-independent nucleosome turnover is higher at Trl- and Mad-binding sites when compared with Sd sites, which could contribute to the relatively greater sensitivity of Sd sites to CAF-1 depletion. Further studies are required, but these findings again suggest that interactions between TFs and chromatin assembly have a complex role in the functioning of signaling pathways in development.

It is important to note that in addition to its role in promoting transcription of Hippo pathway targets, Sd interacts with Tondu-domain-containing Growth Inhibitor to repress pathway targets in the absence of Yki (Koontz *et al.*, 2013). This raises the question of whether nucleosome depletion affects both Sd's default repression function and its transcriptional activation function. While our work does not directly answer this question, it seems likely that Sd interaction with DNA is affected by its binding partner and as a result CAF-1 depletion might not affect Sd's functions in promoting and repressing target site expression in the same way.

Previous studies of Yki function have shown that Yki has the ability to recruit chromatin modifiers, including Trr, to its target genes, thereby promoting increased chromatin accessibility and target gene expression. While these studies provided evidence only for local chromatin alterations at known Yki-binding sites, we took advantage validated antibodies and the internally controlled tissue mosaicism afforded by the Gal4-UAS system to look for subtle but more global effects on histone methylation by tissue staining. Although we

did not observe effects from CAF-1 depletion in the wing imaginal disk on the abundance of activating histone marks, we did observe a marked decrease in repressive methylation marks at H3K27. These results were particularly surprising for the following reasons. First, the effects of CAF-1 depletion on H3K27 methylation were strongly suppressed by heterozygosity for a *yki* null allele, suggesting that these effects are mediated by Yki. This observation suggests that Yki has a more widespread role in regulating chromatin accessibility than previously has been recognized. Second, given published estimates of ~3000 Yki-binding targets in the fly genome (Oh *et al.*, 2013; Zhang *et al.*, 2017), our results suggest that Yki could have an important role in suppressing the spread of repressive marks. Previous work has shown that Yki can promote local recruitment of activating histone marks (Oh *et al.*, 2014; Qing *et al.*, 2014) but has not examined repressive marks. Third, while CAF-1 depletion has widespread effects on repressive histone marks, reduction in these marks does not appear to have widespread transcriptional effects and instead seems to have specific effects on Hippo pathway targets at least in the wing imaginal disk. We do not currently fully understand the role of Yki in regulating chromatin accessibility or the impact of this role in expression of its targets, but these results clearly indicate the importance of further studies to address these questions.

An additional intriguing aspect of our findings is the observation that inhibiting DNA replication suppresses the effects of CAF-1 depletion on Yki target gene expression. This result is consistent with the idea that CAF-1 competes with transcriptional activators, including Yki, as the chromatin reassembles after the replication fork (Ramachandran and Henikoff, 2016). It also raises the question of whether expression of Hippo pathway targets, or specifically changes in expression of those targets, is coupled to DNA replication during normal development. Such coupling could have important implications for Hippo pathway regulation of tissue growth by stabilizing pathway output for the duration of the cell cycle. Alternatively, our observations also raise the possibility that Yki-mediated transcription could be regulated by the cell cycle, perhaps being greatest immediately after S-phase in G2 and relatively quiescent in G1. Elucidation of the precise effects of the competition we have described between the transcriptional coactivator Yki and the nucleosome assembly factor CAF-1 for access to Hippo pathway target genes will require more precise analysis of the transcriptional profiles of these targets.

MATERIALS AND METHODS

Drosophila culture and genetics

All *Drosophila* culture was performed at 25°C unless otherwise noted. For experiments using conditional knockdown or expression, larvae carrying *tubGal80^{TS}* together with a *Gal4* driver (i.e., *hh-Gal4)* were reared at 18°C for 48–72 h and then shifted to 29°C. Late third-instar larvae were then dissected as usual. To induce somatic mosaic clones, larvae were heat shocked 60–84 h after egg laying in a 37°C water bath for 1 h.

The following genotypes of flies were used in this study:

w; UAS-Caf1-180-RNAi-30B/{TubGal80^{TS}}20; Diap1^{j5C8} hh-Gal4

w; UAS-Caf1-180-RNAi-30B/{TubGal80^{TS}}20; hh-Gal4/f-j5.1-LacZ

w, Ubi-mRFP.nls, hs-FLP 19AFRT (BL31418)*/Caf1-180^{270} 19AFRT*

w, Ubi-mRFP.nls, hs-FLP 19AFRT/Caf1-180^{270} 19AFRT; f-j5.1-LacZ

Nub-Gal4

Nub-Gal4/UAS-Caf1-180-RNAi-30B

Nub-Gal4/UAS-Caf1-180-RNAi-30B yki^{B5}

w; UAS-Caf1-105-RNAi (VDRC110461)/{*TubGal80^{TS}*}20; *Diap1^{j5C8} hh-Gal4*

w; UAS-Caf1-55-RNAi (BL31714)/{*TubGal80^{TS}*}20; *Diap1^{j5C8} hh-Gal4*

w; apterous-Gal4; Dad-lacZ (BL11070)*/UAS-Caf1-180-RNAi* (VDRC20151)

w; {TubGal80^{TS}}20; Diap1^{j5C8} hh-Gal4/UAS-yki-RNAi (VDRC40497)

w; UAS-Caf1-180-RNAi-30B/{TubGal80^{TS}}20; Diap1^{j5C8} hh-Gal4/UAS-yki-RNAi

w; UAS-Caf1-105-RNAi/{TubGal80^{TS}}20; Diap1^{j5C8} hh-Gal4/UAS-yki-RNAi

w; {yki-YFP}VK37 nub-Gal4 yki^{B5}

w; {yki-YFP}VK37 nub-Gal4 yki^{B5}/{yki-YFP}VK37 yki^{B5}; UAS-Caf1-180-RNAi

w; {TubGal80^{TS}}20; Diap1^{j5C8} hh-Gal4/UAS-ORC4-RNAi (BL32409)

w; UAS-Caf1-180-RNAi-30B/{TubGal80^{TS}}20; Diap1^{j5C8} hh-Gal4/UAS-Orc4-RNAi

w; {TubGal80^{TS}}20; Diap1^{j5C8} hh-Gal4/UAS-dap

w; UAS-Caf1-180-RNAi-30B/{TubGal80^{TS}}20; Diap1^{j5C8} hh-Gal4/UAS-dap

w; UAS-Caf1-180-RNAi-30B yki^{B5}/{TubGal80^{TS}}20; hh-Gal4, UAS-mRFP

w; UAS-wts-RNAi (VDRC106174); *hh-Gal4, UAS-mRFP*

w; UAS-wts-RNAi/yki^{B5}; hh-Gal4, UAS-mRFP

w Caf1-180-GFP

w Caf1-180-GFP; *UAS-hpo-RNAi* (VDRC104169); *hh-Gal4*

The *UAS-Caf1-180-RNAi-30B* line was subjected to recombination to remove the 40D insertion from VDRC108240 as previously described (Vissers *et al.*, 2016).

The *Caf1-180-GFP* allele was generated using the Scarless CRISPR/Cas9 technique (http://flycrispr.molbio.wisc.edu/scarless). A 1-kb left homology arm containing the 3′ end of *Caf1-180*, msGFP (Fitzgerald and Glick, 2014), and a 1-kb right homology arm containing the first 1-kb genomic sequence downstream of *Caf1-180* were cloned into pHD-ScarlessDsRed (Drosophila Genomics Resources Center). This plasmid was coinjected with a pU6-Bbs1–chiRNA-based plasmid expressing a *Caf1-180* guide sequence (5′-GATGCTCTCGGATTAAGACTAGG-3′) into *vas-Cas9* embryos. In case of successful recombination, the endogenous guide RNA recognition sequence will be disrupted by the GFP sequence. G0 flies were crossed to *w1118* and individual DsRed positive F1s were selected to establish stocks. The DsRed marker cassette was then removed through a single cross to a source of PBac transposase (BL8285). The *Caf1-180-GFP* allele was verified by PCR, sequencing, and live imaging.

Wing imaginal disk immunostaining and in situ hybridization

Wandering third instar larvae were dissected in Schneider's *Drosophila* Medium (Sigma-Aldrich) supplemented with 10% fetal bovine serum to collect wing imaginal disks, which were fixed in 2% paraformaldehyde in PBS for 20 min. Primary antibodies were incubated overnight at 4°C. The following primary antibodies were used: guinea pig anti-Mer (1:10,000) (Lajeunesse *et al.*, 1998), mouse anti-β-galactosidase (1:500, DSHB), mouse anti-CycE (1:10) (Richardson *et al.*, 1995), rabbit anti-H3K27me2 (1:1000, Cell

Signaling Technology), rabbit anti-H3K27me3 (1:1000, Cell Signaling Technology). All secondary antibodies (Jackson ImmunoResearch Laboratories) were used at 1 µg/1 ml. Wing disks were mounted in Prolong Diamond Antifade Mountant (Thermo Fisher Scientific) and subsequently imaged using either a Zeiss LSM 800 or a LSM 880 laser scanning confocal microscope.

Confocal images were processed with ImageJ. To quantify antibody staining intensity, a same area size in the posterior (*hh-Gal4* expression region) and anterior (control region) of each wing blade was selected and quantified using the "Measure" tool. Regions close to the anterior–posterior compartment boundary were avoided because some reporters (i.e., Diap1-lacZ) display increased staining along the border in controls. For Mer staining, a maximum projection of two to four apical sections, where Mer localizes, was used. For Diap1-lacZ and DAPI, a maximum projection of two to four sections more basal sections containing the top portion of the nuclei was used. The average pixel intensity ratio of posterior versus anterior of each disk was calculated and the Student's *t* test was performed between the indicated groups using nonpairwise comparisons.

Wing imaginal disk in situ hybridization was done as described previously (Jemc and Rebay, 2007). To generate a *Mer*-specific RNA probe, a DNA template (base pairs 587–1231 of the *Mer* coding sequence) was amplified by PCR using primers 5′-TAATACGACTCACTATAGGGAGATCCTGGCTGAAAATGGAGAAGCG-3′ and 5′-ATTTAGGTGACACTATAGAAGTGTGGAGGTCCTGCGAGTAAAAG-3′. This template was used with a MEGAscript T7 Transcription Kit (Thermo Fisher Scientific) to synthesize the single-stranded RNA probe.

Expression analysis by qPCR

RNA was extracted from 200 wandering third larvae wing imaginal disks using Direct-zol RNA Miniprep (Zymo Research) with in-column DNAse treatment. RNA (1µg) was used with iScript cDNA Synthesis Kit (Bio-Rad Laboratories) to carry out reverse transcription according to manufacturer's protocol. qPCR was performed using the iTaq Universal SYBR Green Supermix (Bio-Rad Laboratories) on a CFX384 Real-Time PCR Detection System (Bio-Rad Laboratories) in triple technical replicates and subsequently analyzed with manufacturer's CFX Manager software. Primers for qPCR are listed in Supplemental Table S3.

Chromatin immunoprecipitation and downstream analysis

Wing imaginal disk ChIP was done as previously described (Webber *et al.*, 2013) with the following modifications: 200–250 wandering third instar larvae wing imaginal disks were used for each ChIP experiment; a guinea pig anti-GFP (1:2000, this study) was used to immunoprecipitate Yki-YFP; protein A magnetic beads (Thermo Fisher Scientific) were used to capture the guinea pig anti-GFP antibody; DNA was purified using the NucleoSpin Gel and PCR Clean-up Kit (Macherey-Nagel).

ChIP-qPCR was performed using the same reagents and equipment as above. Primers to amplify *Diap1*, *ban, Myc,* and *lz* regulatory regions, as well as *Myc* and *lz* control regions, were published previously (Neto-Silva *et al.*, 2010; Milton *et al.*, 2014; Parker and Struhl, 2015). ChIP signals were calculated as percentage of input for both experiment and no antibody mock controls. Mock control ChIP signal was below or close to the detection limit in the qPCR experiments, and therefore was not presented in the figures.

Post-DNA replication nucleosome change analysis

To evaluate nucleosome changes postreplication, we utilized published MINCE-seq data sets (Ramachandran and Henikoff, 2016) generated from *Drosophila* S2 cells that were either treated with GFP dsRNA (mock, denoted as dsGFP) or *Caf1-105* dsRNA (denoted as dsCaf1). MINCE-seq input measures steady state nucleosome profile, and MINCE-seq pull down measures nucleosome profile within 10 min of passage of the replication fork. The GEO accessions for the four data sets used in the analysis presented in this study are shown in Table 1.

dsGFP	Input	GSM1974514
dsGFP	Pull down	GSM1974515
dsCaf1	Input	GSM1974512
dsCaf1	Pull down	GSM1974513

TABLE 1: GEO accession numbers for the four data sets used in the analysis.

CATCH-IT	Input	GSM763027
CATCH-IT	Pull down	GSM763034

TABLE 2: GEO accession numbers of CATCH-IT data sets used in this study.

For analysis of nucleosome profiles from these data sets, fragments between 134 and 160 base pairs were used. For Figure 5 (B–D), Yki ChIP-binding sites were obtained from GSE38594 (GSE38594_Yki_E8-16.bed.gz). Motifs within ChIP peaks were identified using FIMO (Grant *et al.*, 2011). Motifs were obtained from Fly Factor Survey (Zhu *et al.*, 2011). The center of the nucleosome-depleted region (NDR) around the identified motif was used as the reference position for calculating average nucleosome profiles.

Replication-independent nucleosome turnover analysis

To evaluate replication-independent nucleosome turnover at Yki-binding sites, we used published CATCH-IT data sets (Teves and Henikoff, 2011). Fragments between 120 and 174 base pairs from CATCH-IT input and pull-down data sets were used (data sets listed below). We calculated log 2 ratio of normalized CATCH-IT pull-down read density to normalized CATCH-IT input read density at each 10-base pair interval in the genome. CATCH-IT ratio was calculated ± 50 base pairs around the center of the NDR around the identified motifs of Sd, Mad, and Trl at Yki-binding sites. These sites were same as those used for analysis of MINCE-seq data sets. The GEO accessions of CATCH-IT data sets used in this study are shown in Table 2.

Live Imaging. Live imaging of Caf1-180-GFP was performed as previously described (Xu *et al.*, 2018).

ACKNOWLEDGMENTS

We thank H. Richardson, R. Ward, B. McCartney, A. Ruthenburg, B. Glick, TRiP at Harvard Medical School (National Institutes of Health/National Institute of General Medical Sciences [NIH/NIGMS] R01-GM084947), the Developmental Studies Hybridoma Bank, the Bloomington Drosophila Stock Center, and the Vienna Drosophila Resource Center for reagents and fly stocks used in this study. We thank C. Ferguson, S. Horne-Badovinac, A. Ruthenburg, and members of the Fehon laboratory for helpful discussions and comments on the manuscript. We thank I. Rebay and J. Weber for advice on the in situ hybridization, RT-qPCR, and ChIP experiments. W.B.Y. was in part supported by the Genetics and Regulation Training Grant (T32 GM07197). S.R. was supported by the Howard Hughes Medical Institute (for work in S. Henikoff's laboratory), and the RNA

Bioscience Initiative, University of Colorado School of Medicine. This work was supported by a grant from the National Institutes of Health to R.G.F (NS034783).

REFERENCES

Cheloufi S, Elling U, Hopfgartner B, Jung YL, Murn J, Ninova M, Hubmann M, Badeaux AI, Euong Ang C, Tenen D, *et al*. (2015). The histone chaperone CAF-1 safeguards somatic cell identity. Nature 528, 218–224.

Chiacchiera F, Rossi A, Jammula S, Zanotti M, Pasini D (2016). PRC2 preserves intestinal progenitors and restricts secretory lineage commitment. EMBO J 35, 2301–2314.

Cho E, Feng Y, Rauskolb C, Maitra S, Fehon R, Irvine KD (2006). Delineation of a Fat tumor suppressor pathway. Nat Genet 38, 1142–1150.

De Nooij JC, Letendre MA, Hariharan IK (1996). A cyclin-dependent kinase inhibitor, dacapo, is necessary for timely exit from the cell cycle during Drosophila embryogenesis. Cell 87, 1237–1247.

Dong J, Feldmann G, Huang J, Wu S, Zhang N, Comerford SA, Gayyed MF, Anders RA, Maitra A, Pan D (2007). Elucidation of a universal size-control mechanism in Drosophila and mammals. Cell 130, 1120–1133.

Fei Q, Yang X, Jiang H, Wang Q, Yu Y, Yu Y, Yi W, Zhou S, Chen T, Lu C, *et al*. (2015). SETDB1 modulates PRC2 activity at developmental genes independently of H3K9 trimethylation in mouse ES cells. Genome Res 25, 1325–1335.

Fitzgerald I, Glick BS (2014). Secretion of a foreign protein from budding yeasts is enhanced by cotranslational translocation and by suppression of vacuolar targeting. Microb Cell Fact 13, 1–12.

Grant CE, Bailey TL, Noble WS (2011). FIMO: Scanning for occurrences of a given motif. Bioinformatics 27, 1017–1018.

Hamaratoglu F, Willecke M, Kango-Singh M, Nolo R, Hyun E, Tao C, Jafar-Nejad H, Halder G (2006). The tumour-suppressor genes NF2/Merlin and Expanded act through Hippo signalling to regulate cell proliferation and apoptosis. Nat Cell Biol 8, 27–36.

Huang H, Yu Z, Zhang S, Liang X, Chen J, Li C, Ma J, Jiao R (2010). Drosophila CAF-1 regulates HP1-mediated epigenetic silencing and pericentric heterochromatin stability. J Cell Sci 123, 2853–2861.

Huang J, Wu S, Barrera J, Matthews K, Pan D (2005). The Hippo signaling pathway coordinately regulates cell proliferation and apoptosis by inactivating Yorkie, the Drosophila Homolog of YAP. Cell 122, 421–434.

Jamieson K, Wiles ET, Mcnaught KJ, Sidoli S, Leggett N, Shao Y, Garcia BA, Selker EU (2016). Loss of HP1 causes depletion of H3K27me3 from facultative heterochromatin and gain of H3K27me2 at constitutive heterochromatin. 97–107.

Jemc J, Rebay I (2007). Identification of transcriptional targets of the dual-function transcription factor/phosphatase eyes absent. Dev Biol 310, 416–429.

Kaufman PD, Kobayashi R, Kessler N, Stillman B (1995). The p150 and p60 subunits of chromatin assembly factor I: a molecular link between newly synthesized histones and DNA replication. Cell 81, 1105–1114.

Koontz LM, Liu-Chittenden Y, Yin F, Zheng Y, Yu J, Huang B, Chen Q, Wu S, Pan D (2013). The Hippo effector Yorkie controls normal tissue growth by antagonizing scalloped-mediated default repression. Dev Cell 25, 388–401.

Lajeunesse DR, Mccartney BM, Fehon RG (1998). Structural analysis of Drosophila Merlin reveals functional domains important for growth control and subcellular localization. J Cell Biol 141, 1589–1599.

Le HQ, Ghatak S, Yeung CYC, Tellkamp F, Günschmann C, Dieterich C, Yeroslaviz A, Habermann B, Pombo A, Niessen CM, *et al*. (2016). Mechanical regulation of transcription controls Polycomb-mediated gene silencing during lineage commitment. Nat Cell Biol 18, 864–875.

Lo P, Huang Y, Corcoran D, Jiao R, Deng W (2019). Inhibition of Notch signaling by the p105 and p180 subunits of Drosophila chromatin assembly factor 1 is required for follicle cell proliferation. J Cell Sci 132, jcs224170.

Matakatsu H, Blair SS (2012). Separating planar cell polarity and Hippo pathway activities of the protocadherins Fat and Dachsous. Development 139, 1498–1508.

Milton CC, Grusche FA, Degoutin JL, Yu E, Dai Q, Lai EC (2014). The Hippo pathway regulates hematopoiesis in Drosophila melanogaster. Curr Biol 24, 2673–2680.

Moggs JG, Grandi P, Quivy JP, Jónsson ZO, Hübscher U, Becker PB, Almouzni G (2000). A CAF-1-PCNA-mediated chromatin assembly pathway triggered by sensing DNA damage. Mol Cell Biol 20, 1206–1218.

Murzina N, Verreault A, Laue E, Stillman B (1999). Heterochromatin dynamics in mouse cells: interaction between chromatin assembly factor 1 and HP1 proteins. Mol Cell 4, 529–540.

Nakano S, Stillman B, Horvitz HR (2011). Replication-coupled chromatin assembly generates a neuronal bilateral asymmetry in C. elegans. Cell 147, 1525–1536.

Neto-Silva RM, de Beco S, Johnston LA (2010). Evidence for a growth-stabilizing regulatory feedback mechanism between Myc and Yorkie, the Drosophila homolog of Yap. Dev Cell 19, 507–520.

Oh H, Irvine KD (2008). In vivo regulation of Yorkie phosphorylation and localization. Development 135, 1081–1088.

Oh H, Irvine KD (2011). Cooperative regulation of growth by Yorkie and Mad through bantam. Dev Cell 20, 109–122.

Oh H, Slattery M, Ma L, Crofts A, White KP, Mann RS, Irvine KD (2013). Genome-wide association of Yorkie with chromatin and chromatin-remodeling complexes. Cell Rep 3, 309–318.

Oh H, Slattery M, Ma L, White KP, Mann RS, Irvine KD (2014). Yorkie promotes transcription by recruiting a histone methyltransferase complex. Cell Rep 8, 449–459.

Pan D (2010). The hippo signaling pathway in development and cancer. Dev Cell 19, 491–505.

Parker J, Struhl G (2015). Scaling the Drosophila wing: TOR-dependent target gene access by the Hippo pathway transducer Yorkie. PLoS Biol 13, 1–28.

Qing Y, Yin F, Wang W, Zheng Y, Guo P, Schozer F, Deng H, Pan D (2014). The Hippo effector Yorkie activates transcription by interacting with a histone methyltransferase complex through Ncoa6. Elife 3, e02564.

Ramachandran S, Henikoff S (2016). Transcriptional regulators compete with nucleosomes post-replication. Cell 165, 580–592.

Ray-Gallet D, Woolfe A, Vassias I, Pellentz C, Lacoste N, Puri A, Schultz DC, Pchelintsev NA, Adams PD, Jansen LET, *et al*. (2011). Dynamics of histone H3 deposition in vivo reveal a nucleosome gap-filling mechanism for H3.3 to maintain chromatin integrity. Mol Cell 44, 928–941.

Richardson H, O'Keefe LV, Marty T, Saint R (1995). Ectopic cyclin E expression induces premature entry into S phase and disrupts pattern formation in the Drosophila eye imaginal disc. Development 121, 3371–3379.

Rothbart SB, Dickson BM, Raab JR, Grzybowski AT, Krajewski K, Guo AH, Shanle EK, Josefowicz SZ, Fuchs SM, Allis CD, *et al*. (2015). An interactive database for the assessment of histone antibody specificity. Mol Cell 59, 502–511.

Shibahara K, Stillman B (1999). Replication-dependent marking of DNA by PCNA facilitates CAF-1-coupled inheritance of chromatin. Cell 96, 575–585.

Smith S, Stillman B (1989). Purification and characterization of CAF-I, a human cell factor required for chromatin assembly during DNA replication in vitro. Cell 58, 15–25.

Sopko R, Silva E, Clayton L, Gardano L, Barrios-Rodiles M, Wrana J, Varelas X, Arbouzova NI, Shaw S, Saburi S, *et al*. (2009). Phosphorylation of the tumor suppressor Fat is regulated by its ligand Dachsous and the kinase discs Overgrown. Curr Biol 19, 1112–1117.

Su T, Ludwig MZ, Xu J, Fehon RG (2017). Kibra and Merlin activate the Hippo pathway spatially distinct from and independent of Expanded. Dev Cell 40, 478–490.e3.

Subbanna S, Shivakumar M, Umapathy NS, Saito M, Mohan PS, Kumar A, Nixon RA, Verin AD, Psychoyos D, Basavarajappa BS (2013). G9a-mediated histone methylation regulates ethanol-induced neurodegeneration in the neonatal mouse brain. Neurobiol Dis 54, 475–485.

Teves SS, Henikoff S (2011). Heat shock reduces stalled RNA polymerase II and nucleosome turnover genome-wide. Genes Dev 25, 2387–2397.

Vissers JHA, Manning SA, Kulkarni A, Harvey KF (2016). A Drosophila RNAi library modulates Hippo pathway-dependent tissue growth. Nat Commun 7, 1–6.

Webber JL, Zhang J, Cote L, Vivekanand P, Ni X, Zhou J, Nègre N, Carthew RW, White KP, Rebay I (2013). The relationship between long-range chromatin occupancy and polymerization of the drosophila ets family transcriptional repressor yan. Genetics 193, 633–649.

Wu S, Liu Y, Zheng Y, Dong J, Pan D (2008). The TEAD/TEF family protein Scalloped mediates transcriptional output of the Hippo growth-regulatory pathway. Dev Cell 14, 388–398.

Xu J, Vanderzalm PJ, Ludwig M, Su T, Tokamov SA, Fehon RG (2018). Yorkie functions at the cell cortex to promote myosin activation in a non-transcriptional manner. Dev Cell 46, 271–284.e5.

Xuan T, Xin T, He J, Tan J, Gao Y, Feng S, He L, Zhao G, Li M (2013). DBre1/dSet1-dependent pathway for histone H3K4 trimethylation has essential

roles in controlling germline stem cell maintenance and germ cell differentiation in the Drosophila ovary. Dev Biol 379, 167–181.
Yu Z, Wu H, Chen H, Wang R, Liang X, Liu J, Li C, Deng W-M, Jiao R (2013). CAF-1 promotes Notch signaling through epigenetic control of target gene expression during Drosophila development. Development 140, 3635–3644.
Zhang L, Ren F, Zhang Q, Chen Y, Wang B, Jiang J (2008). The TEAD/TEF family of transcription factor Scalloped mediates Hippo signaling in organ size control. Dev Cell 14, 377–387.
Zhang P, Pei C, Wang X, Xiang J, Sun B, Cheng Y, Qi X, Marchetti M, Xu J-W, Sun Y, *et al.* (2017). A balance of Yki/Sd activator and E2F1/Sd repressor complexes controls cell survival and affects organ size. Dev Cell 43, 603–617.e5.
Zhu LJ, Christensen RG, Kazemian M, Hull CJ, Enuameh MS, Basciotta MD, Brasefield JA, Zhu C, Asriyan Y, Lapointe DS, *et al.* (2011). FlyFactorSurvey: a database of Drosophila transcription factor binding specificities determined using the bacterial one-hybrid system. Nucleic Acids Res 39, 111–117.